

# Assessing and Delineation of Groundwater Recharge Areas in Coastal Arid Area in Tunisia Using GIS, Remote Sensing Techniques and Self-organizing Map

Bilel Abdelkarim (✉ [abdalebilel92@gmail.com](mailto:abdalebilel92@gmail.com))

University of Gabes: Universite de Gabes

Faten Telahigue

University of Gabes: Universite de Gabes

Belgacem Agoubi

University of Gabes: Universite de Gabes

---

## Research Article

**Keywords:** potential recharge, self-organizing maps, arid zones, GIS approach, Gabes

**Posted Date:** January 7th, 2022

**DOI:** <https://doi.org/10.21203/rs.3.rs-1160687/v1>

**License:** © ⓘ This work is licensed under a Creative Commons Attribution 4.0 International License.

[Read Full License](#)

---

1 **Assessing and delineation of groundwater recharge areas in coastal arid**  
2 **area in Tunisia using GIS, Remote sensing techniques and Self-organizing**  
3 **map**

4  
5 **Bilel Abdelkarim<sup>1</sup>, Faten Telahigue<sup>2</sup>, Belgacem Agoubi<sup>3</sup>**

6 <sup>1,2,3</sup>*Institut Supérieur des Sciences et Techniques des Eaux de Gabès, Université de Gabès,*  
7 *Gabès, Tunisia. LR: Applied Hydro-Sciences Laboratory research*

8 *Campus universitaire, 6072 Zrig, Gabes, Tunisia*

9  
10 *\*Corresponding author: Bilel Abdelkarim*

11 *E-mail: abdelbilel92@gmail.com*

12  
13 **Abstract**

14 In Gabès region (southeastern Tunisia), given the semi-arid to arid climate conditions,  
15 groundwater is an essential resource to supply the growth needs of the socio-economic  
16 development. To ensure sustainable development and preserve–water resources, a careful  
17 estimation of the present day recharge amount and the delineation of the potential zones of  
18 rainfall precipitation are of required for an accurate evaluation of regional water balance. In this  
19 context, this study aims to a preliminary assessment of groundwater recharge in Gabes basin in  
20 regard to the delineation of the potential recharge areas of phreatic aquifers. Thus, a geological  
21 and hydrogeological collected database coupled with remote sensing techniques (RST) were

22 used for the determination of the lateral variation of recharging zone ,Treatment by ArcGIS and  
23 Matlab softwares and Kohonen self-organizing maps (K-SOM) approaches.

24 The obtained results indicate that five recharge potential areas have been identified and  
25 classified as 27% very low, 23% low, 40% moderate recharge, 7% good and 3 % very good  
26 potential recharge located principally on southern part of the study region .This distribution is  
27 controlled principally by the geomorphological, geologic, and hydrogeologic features of the  
28 region . Reasonable management strategies based on a perennial exploitation of these low  
29 renewable resources are required to optimize the water dependent socio-economic  
30 development. The estimated groundwater potential recharge of Gabès aquifer system using K-  
31 SOM and RST is of  $11.4 \text{ Mm}^3 \cdot \text{y}^{-1}$ . This recharging rate is very low it present 7% of the total  
32 rain, thus it must be ameliorated. K-SOM and RST approach is a useful method for groundwater  
33 potential recharge mapping and is a helpful of wells establishment and groundwater sustainable  
34 management.an isotopic analyses is recommended to ameliorate the decision maker to establish  
35 the adequate strategy.

36

37 **Key words:** potential recharge, self-organizing maps, arid zones, GIS approach, Gabes.

38

## 39 **1. Introduction**

40 Groundwater is the lifeblood of arid and semi-arid areas regarding to the lack of surface  
41 water and the rain scarcity. The limited fresh groundwater resources are continuously supplied  
42 to meet the growing demands of expansion economic activities and growing population. These  
43 deep confined and semi-confined aquifers, generally low renewable under present day climate  
44 conditions, have an important impact on ecosystems, well-being, societal growth and economic  
45 development (Hamed et al 2018, Parkinson et al 2020, Agoubi 2021). Under the combined effect

46 of socio- economic conditions, climate variability and emerging consumption patterns, world  
47 water use has been increasing annually by about 1% since the 1980s (UNESCO, 2019) and  
48 global water demand is expected to continue increasing to meet domestic, agricultural and  
49 industrial needs.

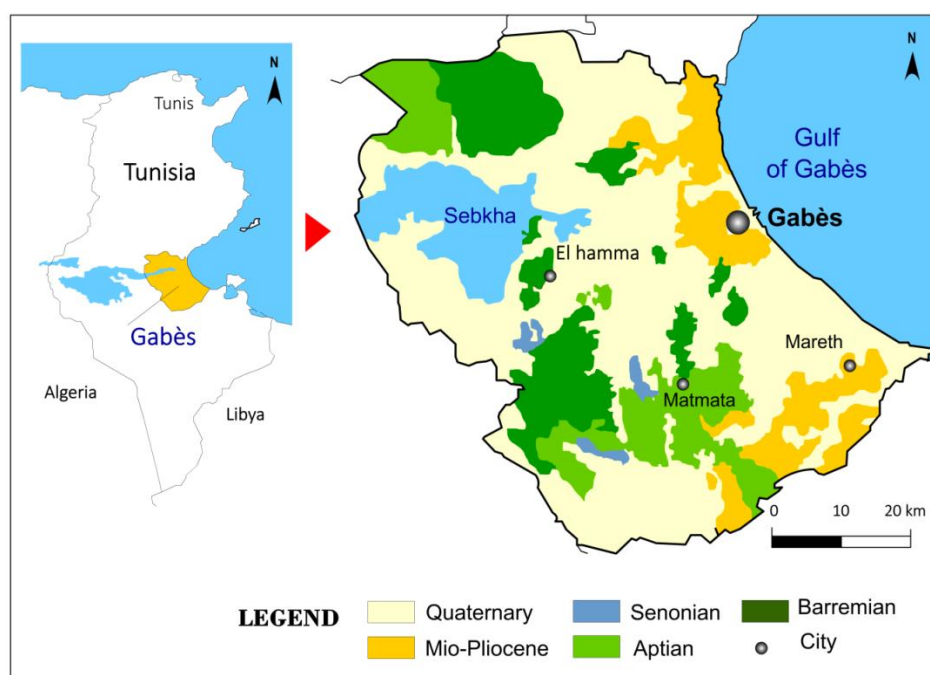
50 The excessive exploitation of groundwater resources has led to many environmental issues  
51 challenging the sustainable use of these reservoirs (Kulmatov et al 2020, Pool et al 2021).  
52 Water withdrawal, aquifer decompression, water quality salinization and chemical evolution,  
53 pollution, are the commonly observed problems in many water-deficit regions, especially in  
54 developing countries, for example in Algeria(Bouderbala et al 2019) , in Iraq (Awadh et al  
55 2021) and in Australia(Akbari et al 2020) .A reasonable management of these limited highly  
56 solicited resources is required. The adopted strategies may rely on a systematic monitoring of  
57 water quality and quantity evolution in the light of the available freshwater amount related to  
58 aquifer characteristics and the local and regional geological and hydrogeological context (Gude  
59 et al 2018, Nadiri et al 2019).Identifying and protecting potential groundwater recharge areas,  
60 and adopting proactive solutions to preserve the collected surface water volume, are the most  
61 feasible low expensive, and easy to implant remediation actions(Nadiri et al 2019). Indeed,  
62 potential recharge areas delineation is of paramount importance for aquifers management  
63 discussed by zones has been a subject of several works under different weather features and  
64 socio-economic conditions (Lee and Jones-Lee 1999; Mishra et al. 2010; Najib et al. 2018;  
65 Singh et al., 2019; Dar et al. 2020; Balamurugan et al., 2017; Yahyaoui et al. 2021). These  
66 studies confirmed that potential groundwater area mapping is not trivial task due to the large  
67 parameters number influencing the recharge process. In fact, groundwater recharge estimation  
68 is governed by several factors such as geology, precipitation and geomorphology (yeh et al  
69 2016, Suissi et al 2018, Yahyaoui et al 2021).These works have, furthermore, adopted various  
70 methods based on geographic information system (GIS) and remote sensing techniques among

71 other techniques to assess and classify potential recharge areas (yeh et al 2016, Nadiri et al  
72 2019). The remote sensing techniques to assess groundwater potential recharge zone are used  
73 in several study all over the world; as example in India case study (Arulbalaji et al. 2019, Singh  
74 et al. 2019), in New Zealand (Dar et al. 2020).Yahyaoui et al., (2021) developed the  
75 groundwater potential recharge Index (GPRI) to identify potential recharge areas and to assess  
76 groundwater recharge in Ghomrassen region in Tunisia. In other side ,many others techniques  
77 have been used digital data processing and artificial intelligence techniques such as artificial  
78 neural network (ANN), random forest model (RFM), tree analysis model (TDM) and linear and  
79 logistic regression (LLR) in several works such as, Lee and Jones Lee (1999) , Portaji and  
80 Borjasimi (2014) and Golkarian and Rahmaty (2018).The development of informational data  
81 processing technologies contributed rapidly to the use of digital methods which are becoming  
82 more available and commonly used for useful to hydrogeological researchers.This new  
83 techniques have contributed to the adoption of digital applications and to the improvement of  
84 scientific results qualities. Among the various tools that may be used for water resources  
85 mapping, the Kohonen self-organizing maps (K-SOM) (Kohonen 1982) constitutes a useful  
86 approach that consist to result the hydrogeology and hydrology problems by classifying the  
87 environmental and climate data. This mothed has been used in numerous study such as in  
88 ground water salinization and mixing (Agoubi et al 2018), water quality index (Tison et al.  
89 2004; Kangur et al.2007).However, despite the important potential performance of this  
90 approach especially if it is coupled with supervised learning machine techniques, the K-SOM  
91 is still limited for recharge zones mapping (Kangur et al., 2007; Hsu and Li, 2010; Agoubi,  
92 2018), and produced some very useful results. Various studies have evaluated groundwater  
93 recharge mapping in Tunisia by assigning of remote sensing tools to identify the pentantial  
94 recharge zones (Suissi et al 2018, Yahyaoui et al 2021), but there is no study in the literature  
95 that applies a K-SOM method based in remote sensing tool in that context. Thus, the objective

106 of this work is to develop an approach for the delineation of potential groundwater recharge  
 107 areas in which K-SOM techniques were combined to remote sensing techniques based on  
 108 Shuttle Topography Mission (SRTM) data. A geological and hydrogeological database will be  
 109 implemented to create a potential groundwater recharge map. Thus the main aims of the  
 110 estimation of groundwater recharge were :( 1) characterize the recharge area in the study region  
 111 ;(2) discuss the adequate strategy used to valorize the most of groundwater recharging.

## 102 2. Study area

103 This study is carried out in the Gabès region, southeastern Tunisia (**Fig. 1**). This area is  
 104 characterized by a Mediterranean climate in the coastal area with an annual average of 200  
 105 mm.year<sup>-1</sup>, whereas the western part is affected by an arid climate, dry and hot in the summer  
 106 and wet and cool in the winter, with an annual precipitations do not exceed 150 mm.year<sup>-1</sup>  
 107 (Ben Alaya et al., 2013; Agoubi, 2018). Gabès region is characterized by no perennial rivers;  
 108 however, heavy storms can create surface runoff, which is discharged via wadis such as Oued  
 109 El Akarit, Oued jir and Oued El Hamma (Ben Alaya et al 2013, Agoubi et al 2018).



110

111

**Fig.1** Location map and geological settings of study area

112

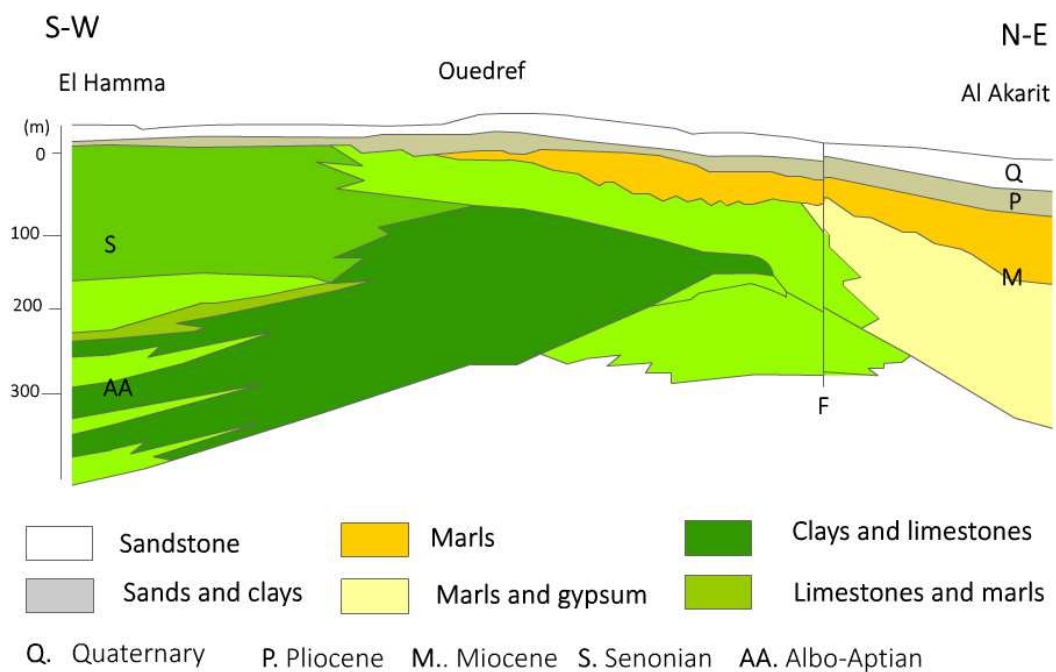
113 ***Geological setting***

114 The studied region is located in the eastern boundary of the Tunisian meridional Atlas. From  
115 a geological point of view, the study area characterized by the exposure of cretaceous and  
116 quaternary layers in surface (fig. 1). Tectonically, the study area constitutes a transition zone  
117 between the Dahar plateau from south-western and the jeffara-platform from the coastal zone.  
118 Furthermore, it characterized by the presence of salt depressions (Fejjj chotts) (Zargouni 1985;  
119 Bouaziz et al. 2002).in addition ,the tectonic features present a multidirectional faults ; E–W  
120 normal Chotts fault, NW–SE Gafsa made a horsts and graben (Mamou 1990,Zouaghi et  
121 al. 2011). Due to these tectonic deformation, the permo-trassic substratum is brought up to  
122 very near the soil surface. The layers slant in the direction of the Mediterranean and get thicker  
123 elsewhere (Bouaziz, 1995). In the study area, Cretaceous formations were composed by  
124 Turonian and Albian. Thereby, the Barremian, is formed by gypsums, clay and anhydrite (Ben  
125 Hammouda et al., 2013). Whereas, the Albian is represented by dolomite, limestone and marl.  
126 The Turonian crops out southeastern part, and is composed of dolomite. The Mio-Pliocene is  
127 represented by gypsum, clays and sands. Finally, the Quaternary covers the region by clays  
128 with a crust of gypsum (**Fig. 2**).

129 ***Hydrogeological setting***

130 In the Mediterranean coastal area of study area, the hydrogeological system of the area is made  
131 of different aquifers systems. According to the lateral variation and the tectonic accident, those  
132 aquifers are interconnected (lateral and vertical).in addition, the deferent reservoirs which are  
133 exploited in Gabes region are logged in the quaternary alluvium and in the cretaceous deposit.  
134 The shallow aquifer is hosted in the sandy clays of Mio-Pliocene deposits, whereas the  
135 Senonian is composed by two stratigraphic units represented by limestone and marly limestone

136 units (Sahli et al., 2013). In the continental western part of study area, the main aquifers were  
 137 logged in the cretaceous deposits such as the thermal continental intercalary and the jeffara  
 138 aquifer (fig.2). The Senonian aquifer, hosted limestone and thermal continental intercalary (CI)  
 139 logged in continental sandstone-clay formations (ben Alaya et al 2013, ben Mahmoud 2015).  
 140 In other hand, the jeffara aquifers was formed in the upper cretaceous formations (Makni et al  
 141 2012, Agoubi et al 2018).those aquifers faced a dropdown in the Piezometric level due to the  
 142 low recharge process and the overexploitation of those resources in industry agriculture and  
 143 human activities(ben Hammouda et al 2013,ben Mahmoud 2015).



144

145

146 **Fig. 2** Geological cross section (A-A') over study area (After Ben Hammouda et al. 2013,  
 147 modified)

148 **3. Methodology**

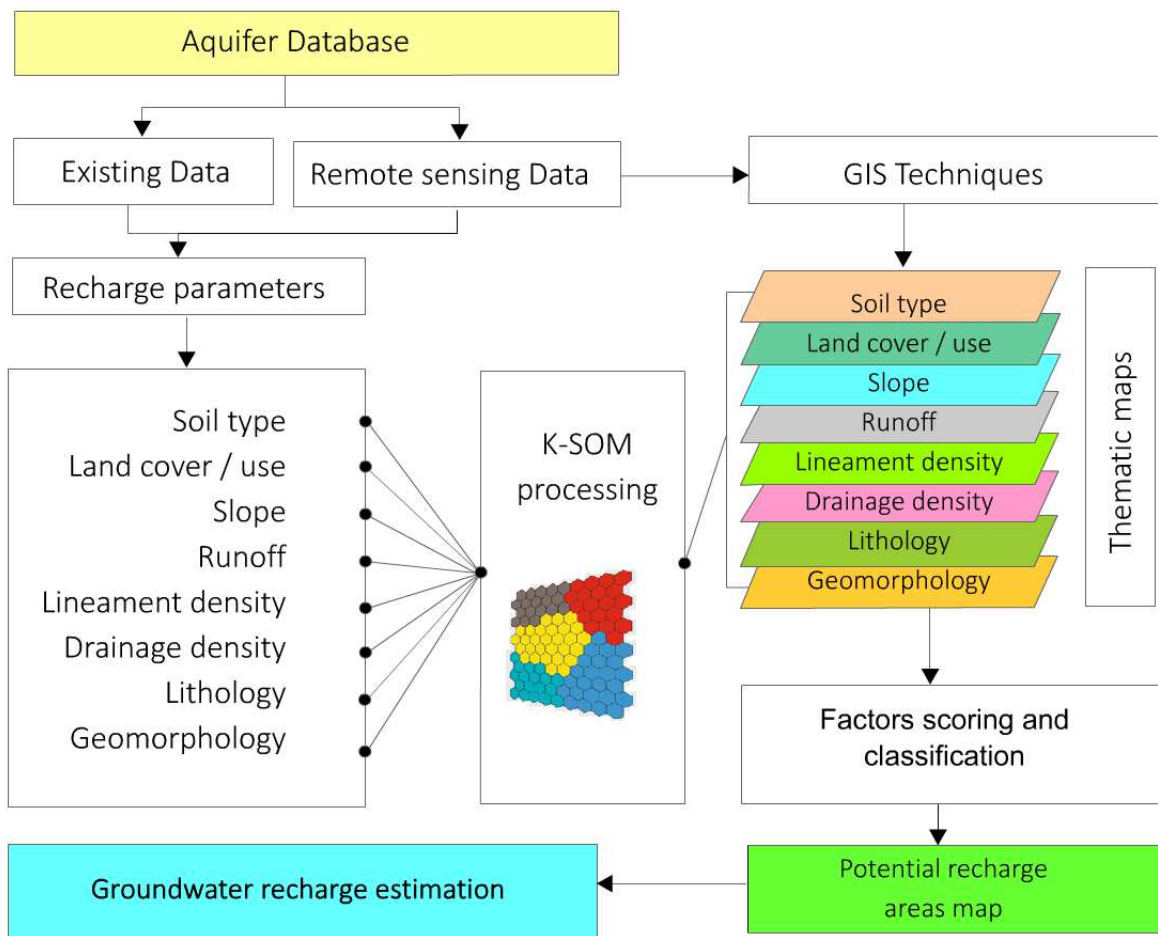
149 **3.1. Factors controlling groundwater recharge**

150 Topography, lithology, geological features, groundwater depth, widespread cracks, primary  
151 porosity, secondary porosity, slope, drainage , land use and cover, and climate presented some  
152 of the variables that influence the presence and groundwater flow in a given region.  
153 Hydrogeology experiments and on-site geophysical studies help explain the groundwater  
154 recharge process and assess spatial-temporal differences in study regions (Abdollahi et al.,  
155 2015; .Malki et al. 2017).

156 As shown in figure 3, the methodology used in this study focused on groundwater potential  
157 recharge areas delineation using K-SOM method integrated remote sensing and GIS techniques.  
158 However, in order to delineate groundwater potential recharge areas, a database including  
159 geological, hydrogeological and topographic data was implemented. In this study, eight  
160 parameters were considered to assess groundwater potential areas: soil type, Land cover/use,  
161 slope, runoff, density of lineament, drainage density, lithology and geomorphology.

162 The lithological map was prepared by assembling, geo-referencing and digitizing local  
163 geological maps. The land-use and cover data were obtained through the Landsat 8 satellite  
164 images processing and then converted into raster format (30-m resolution).

165 The spatial pattern of the different factors estimated by K-SOM method will be presented with  
166 ArcGIS shown the lateral variations of the different parameters to identify regions in the study  
167 area where potential recharge zone may exist.



168

169

**Fig. 3** Flowchart of groundwater potential index computation and mapping

170

### 171 **3.2. Parameters influencing groundwater recharge**

172 The main parameters influencing groundwater recharge were grouped in into three groups. The  
 173 first parameter groups is the physiographic parameters (slope, lineament density,  
 174 geomorphology, lithology); the second is the climatic parameters (runoff, drainage density) and  
 175 the environmental parameters is the third group involved soil type and land cover-use. All the  
 176 parameters considered in this study as well as the role and influence of each parameter on  
 177 recharging will be detailed in what follows.

178 **Soil type:** The soil type parameter has an important influence on water infiltration. So, the soil  
 179 types will be grouped and classified into numerous classes on the basis of texture, thickness,

180 drainage state, and water transmission capacity (Viessman et al., 1989). In recent literature,  
181 soil are classified into three classes such as Sandy and sandy silt, Sandy clay and silt, and Clay,  
182 sandy clay. For each soil class a weight will be assigned.

183 **Land cover -use** : This parameter is one of the most important factors influencing and affect  
184 groundwater recharge. Land cover such as residential areas and vegetation cover controls the  
185 groundwater recharge. Leduc et al., (2001) indicated that groundwater recharge is affected by  
186 land utilization and vegetation cover. Thereby, land-use classes will be deciphered from  
187 Landsat 8 OLI/TIRS satellite images.

188 **Slope** : Groundwater recharge is affected by slope (Al Saud et al. 2010; El-Baz, 1995;  
189 Machiwal et al. 2011; Choi et al. 2012). Due to the substantial high accumulation of rainwater,  
190 low slopes promote groundwater recharge. The slope variance is assessed by the slope analysis  
191 function of GIS using data from the Tunisian digital terrain.

192 **Runoff** : Runoff is the unique source of water recharge in arid and semi- arid aeras. The  
193 runoff assessment depends on outcrop lithology in study area, which provides an important  
194 index of percolation (Trabelssi et al 2009). The runoff is estimated as follow [1]:

$$195 \quad R = 0.0164 P \sqrt{I_g} \quad [1]$$

196 Where, R is the runoff, p: is the mean of precipitation and  $I_g$  is the slope.  
197

198 **Lineament density**: Lineament density parameter is a critical in groundwater recharge  
199 assessment and delineation. Lineament (Faults, fractures, and discontinuity surfaces) provides  
200 the groundwater flow pathways (Abdalla 2012). The STRM dataset and geological map were  
201 used to produce lineament in the study area using the Geomatica 2015 platform. The density of  
202 lineaments is calculated as follows [2], in which  $L_i$  is the length of each network portion and A  
203 is its surface.

$$204 \quad L_d = \frac{\sum_1^n L_i}{A} \quad [2]$$

205 **Drainage density:** Drainage network factor is an important parameter for groundwater  
206 recharge assessment. Thus, groundwater infiltration rate is more important in the highest  
207 runoff density region (Huang et al. 2013). Drainage network was generated from the  
208 topographic map using ArcHydro 10.8 software. This factor is computed as follows [3] where  
209  $S_i$  is the length of  $i$ th drainage network and  $A$  is the surface of studied area.

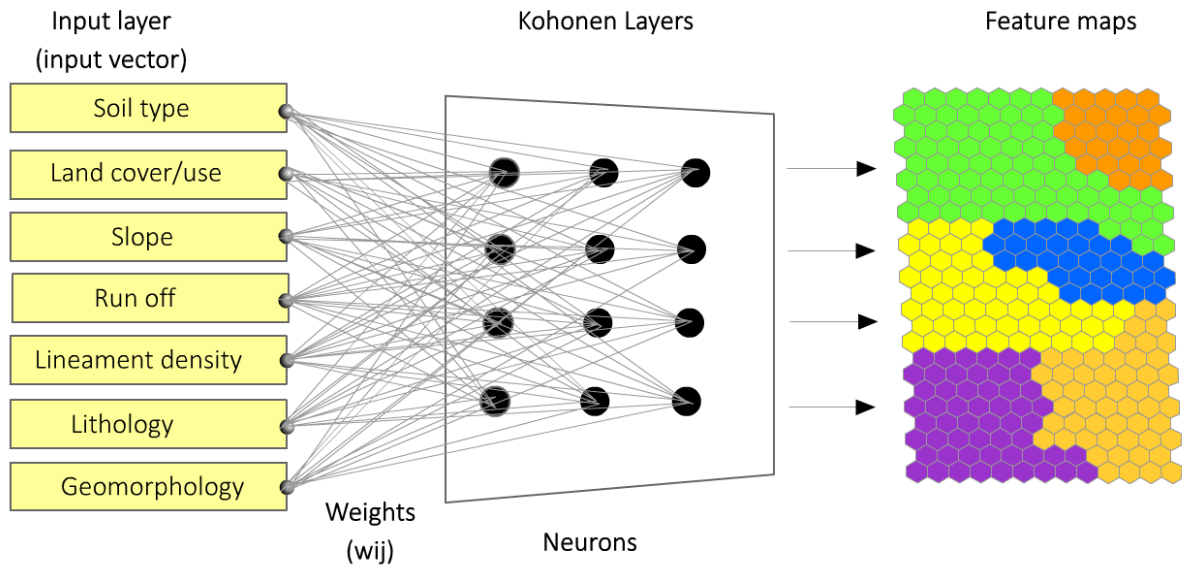
$$210 \quad D_d = \frac{\sum_{i=1}^N S_i}{A} \quad [3]$$

211 **Lithology:** The lithology affects significantly water infiltration (El-Baz, 1995; Yeh et al. 2009;  
212 Oikonomidis et al. 2015). The geological map 1:100000 of the study area will be used to assess  
213 the lithology variation.

214 **Geomorphology:** The geomorphology of the study area plays an important role in water  
215 distribution and availability and helps to identify potential groundwater recharge areas.  
216 Therefore, alluvial plain and low slopes help a great deal in groundwater infiltration due to  
217 their high porosity and permeability.

### 218 **3.3 Kohonen's self-organizing map analysis**

219 Kohonen's self-organizing map (K-SOM) is an unsupervised artificial neural network  
220 (Cereghino and Park, 2009) designed by Kohonen (1982). Several authors such as (Cereghino  
221 and Park, 2009; Clark, 2018) describe K-SOM as an excellent technique for high-dimensional  
222 data visualization that decreases map dimensions (1 or 2) by grouping related data items  
223 together. The self-organizing map presents one of the most prominent neural network models  
224 (Fig. 4). The K-SOM is an unsupervised learning machine and required a limited amount of  
225 information as input data. It has the property of preserving topology data as well as the distance  
226 between them (Vesanto and Alhonen, 2000; Ousmana et al., 2016; Clark, 2018).



227

228

**Fig. 4** Architecture of Kohonen Self-organizing map neural network

229

The Kohonen self-organizing map algorithm uses the distance between the best-matching unit

230

(BMU) and each data point to calculate error .The proportion of data using two BMUs that are

231

not contiguous is calculated by K-SOM as topographic error (Kohonen 1982). In Kohonen

232

maps, the neighborhood function  $h_j(k,t)$  is a continuous Gaussian function (**Fig. 5**). The

233

standard deviation is reduced, resulting in a reduction in the size of the neighborhood (t). The

234

speed of learning is controlled by the learning step (x), whereas the convergence condition is

235

based on standard deviation (t).  $\varepsilon(x)$  and  $\sigma(x)$  are calculated using the formulas [1] and [2],

236

respectively.

237

$$\varepsilon(x) = \varepsilon_i \left( \frac{\varepsilon_f}{\varepsilon_i} \right)^{1/(t \max)} \quad [1]$$

238

$$\sigma(x) = \sigma_i \left( \frac{\sigma_f}{\sigma_i} \right)^{1/(t \max)} \quad [2]$$

239

The topological error (Te) and quantization error (Qe) criteria are used to validate the SOM

240

classification. Te is a criterion for describing how the SOM maintains data topology. The data

241

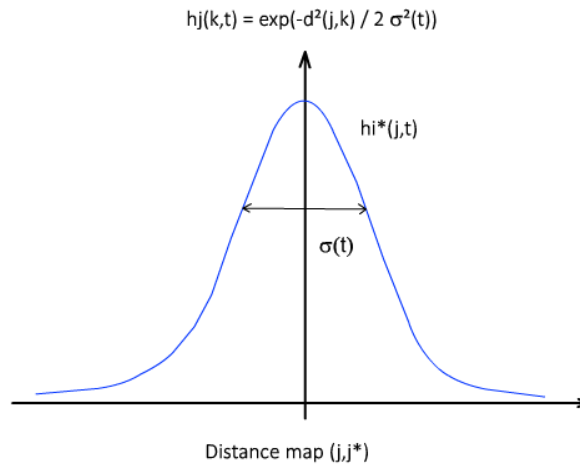
percent of the first two non-adjacent BMUs is measured. Qe is the distance between data and

242

BMU (Kohonen 2001). Qe is computed as follow [3]:

243 
$$Q_e = \frac{1}{N} \sum_{i=1}^N \|X^i - W(X^i)\|^2 \quad [3]$$

244 In which N is the number of dataset,  $i$  is the  $i^{th}$  individual, and  $w(x^i)$  is the best-matching unit  
 245 of the individual.

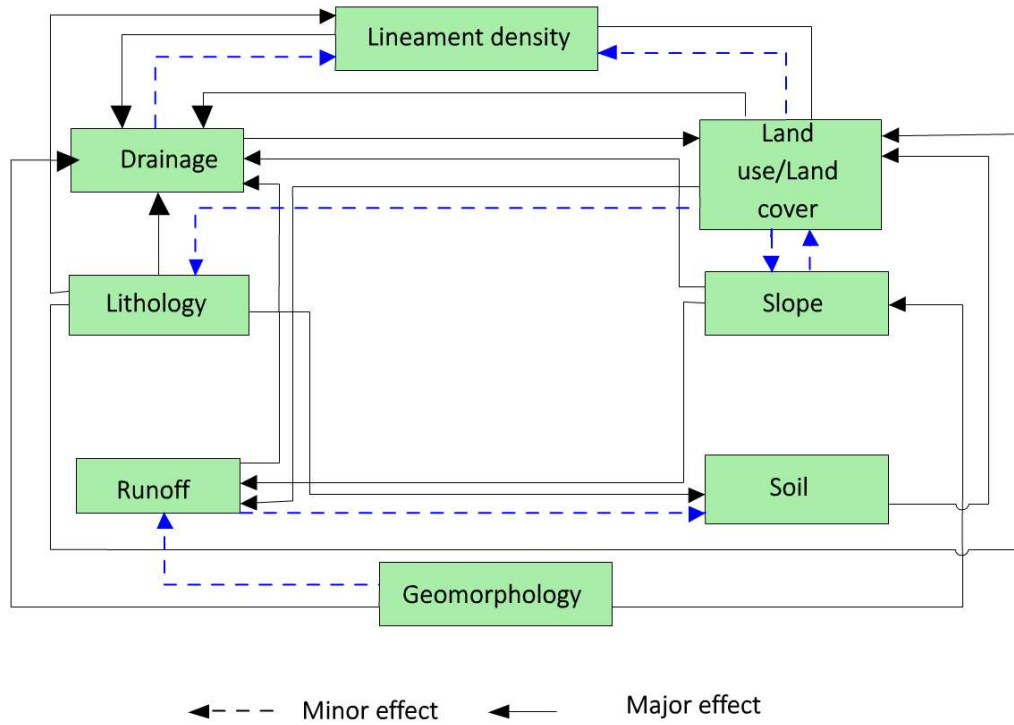


246

247 **Fig. 5** Gaussian function neighborhood used by K-SOM

248 **3.4 Factor's and rating system**

249 The infiltration rate is used to assess factors governing groundwater potential recharge. The  
 250 chosen parameters were rated and a score from 1 to 10 is assigned for each parameter (Table  
 251 1). According to previous studies such as Yeh et al. (2016), Dar et al. (2020), factors namely  
 252 slope, lithology, land use, land cover, drainage density, lineaments density, and runoff were  
 253 rated from 1 to 8 in terms of their contribution to groundwater recharge. The fusion of these  
 254 parameters is represented by the final potential recharge map of the study area. The integration  
 255 of different factors and their causality links were taken into account while calculating the  
 256 potential recharge used to estimate groundwater recharge as the factor weight is assessed using  
 257 inter-parameter relationship effects (Fig. 6).



258

259 **Fig. 6** Relations and effects inter-parameters controlling potential groundwater recharge  
 260 (after, Singh et al. 2019)

261 The major effect is scored 1 and indicates a significant influence, whereas the weight 0.5 is  
 262 affected to the minor effect (Table 2), as follow [4]:

263 
$$score = \frac{(Major\ effect + Minor\ effect)}{\Sigma(Major\ effect + Minor\ effect)} * 100$$
 [4]

264

**Table 1** weights and rates of factors used for assess groundwater potential recharge

Recharge - factor	Value ranges (V)	Weight (w)	Rates (R)	weighted rating (w.R)	Sum	Classes
<b>Land cover - use</b>	Dry land	8	2.5	20	47.5	Very good
	Agriculture	6		15		Good
	Bare land	4		10		Moderate
	Urban zone	1		2.5		Poor
<b>Slope / Topography</b>	<2°	6		15	47.5	Very good
	2 tyo 4°	5		12.5		Good
	4 to 10°	4	2.5	10		Moderate
	10 to 15°	3		7.5		Poor
	>15°	1		2.5		Extremely Poor
<b>Aquifer lithology</b>	Marl and limestone	1		6	88	Extremely Poor
	Silt and clay	2		8		Medium
	Alluvium	5		20		Good
	Sandy clay to sand	4	4	16		Moderate
	Sand	6		24		Very good
<b>Geomorphology</b>	<110	6		12	28	Good
	110–660	2	2	4		Moderate
	Rivers	6		12		Very good
<b>Drainage density</b>	<1	2		3	22.5	Low
	1 to 1.5	3	1.5	4.5		Moderate
	1.5 to 2.5	4		6		Good
	>2.5	6		9		Excellent
<b>Soil type</b>	Sandy and sandy silt	6	1	6	8	Good
	Sandy + clay and silt	2		2		Moderate
	Clay, sandy clay	0		0		Poor
<b>Lineament density (km/km<sup>2</sup>)</b>	>1.5	10	2	20	42	Very good
	1 – 1.5	6		12		Good
	0.5 - 1	4		8		Moderate
	<0.5	1		2		Poor
<b>Runoff</b>	<4 %	10		25	67.5	Very good
	4 - 20%	8		20		Good
	20 - 35%	5	2.5	12.5		Moderate
	35 - 50%	3		7.5		Poor
	>50%	1		2.5		Extremely Poor

267 **Table 2.** Parameters assigned scores (after, Singh et al. 2019)

Parameter	Significant effect	slight effect	Rate calculation	Rate	Score
Lithology	4	0	$(4 \times 1) + (0 \times 0.5)$	4	19
Lineament density (km/km <sup>2</sup> )	2	0	$2 + (0 \times 0.5)$	2	10
Geomorphology	2	0	$(2 \times 1) + (0 \times 0.5)$	2	10
Slope	2	1	$(2 \times 1) + (1 \times 0.5)$	2.5	14
Land cover	1	3	$(1 \times 1) + (3 \times 0.5)$	2.5	19
Drainage density	1	1	$(1 \times 1) + (1 \times 0.5)$	1.5	10
Runoff	2	1	$(2 \times 1) + (1 \times 0.5)$	2.5	14
Soil	1	0	$(1 \times 1) + (0 \times 0.5)$	1	5

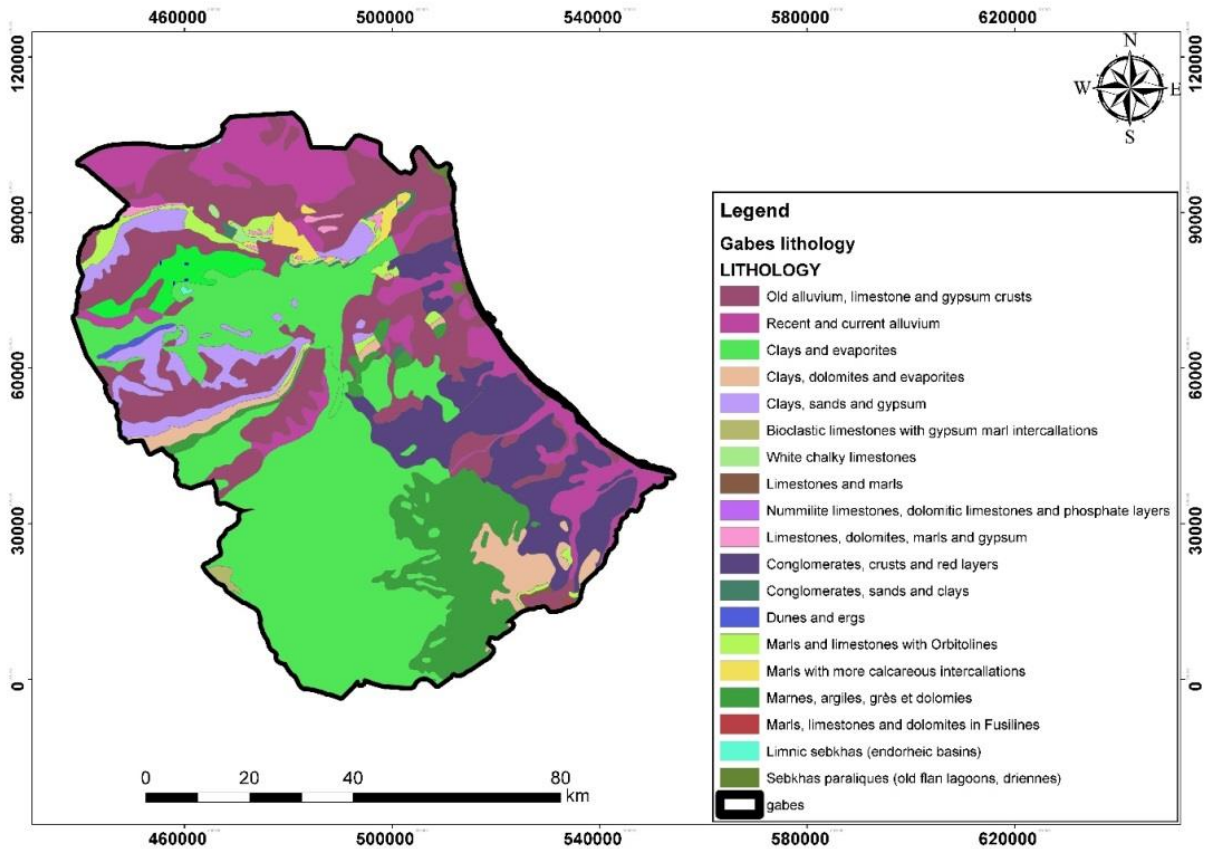
268

269 **4. Results and discussion**

270 **Lithology**

271 Groundwater recharge is affected by lateral and vertical changes of strata. It has been pointed  
 272 out by several researchers (Yeh et al., 2009) that the lithology of the near surface formations  
 273 impact the potential recharge amount of groundwater resources. The physic-chemical  
 274 proprieties of these deposits influence furthermore the recharge potential namely porosity and  
 275 permeability (Oikonomidis et al. 2015, Welter.2018). This research includes rock variation  
 276 that may alter lineages and morphology.

277 The Gabes district is overlain by alluvium and Quaternary sediments, which account for nearly  
 278 70% of the absolute region, according to the lithology map (**Fig. 7**). In the study area, the  
 279 Lower Pleistocene and Pliocene are represented by sands and conglomerates which  
 280 characterize by a moderate permeability and porosity important to the recharge phenomena.  
 281 The Miocene is composed of coarse sand. Limestone marls and Cretaceous dolomite cover the  
 282 reliefs, that variability of lithology layers may can minimize the infiltration rate. The lithology  
 283 parameter represents 25% of the potential recharge of the study area.

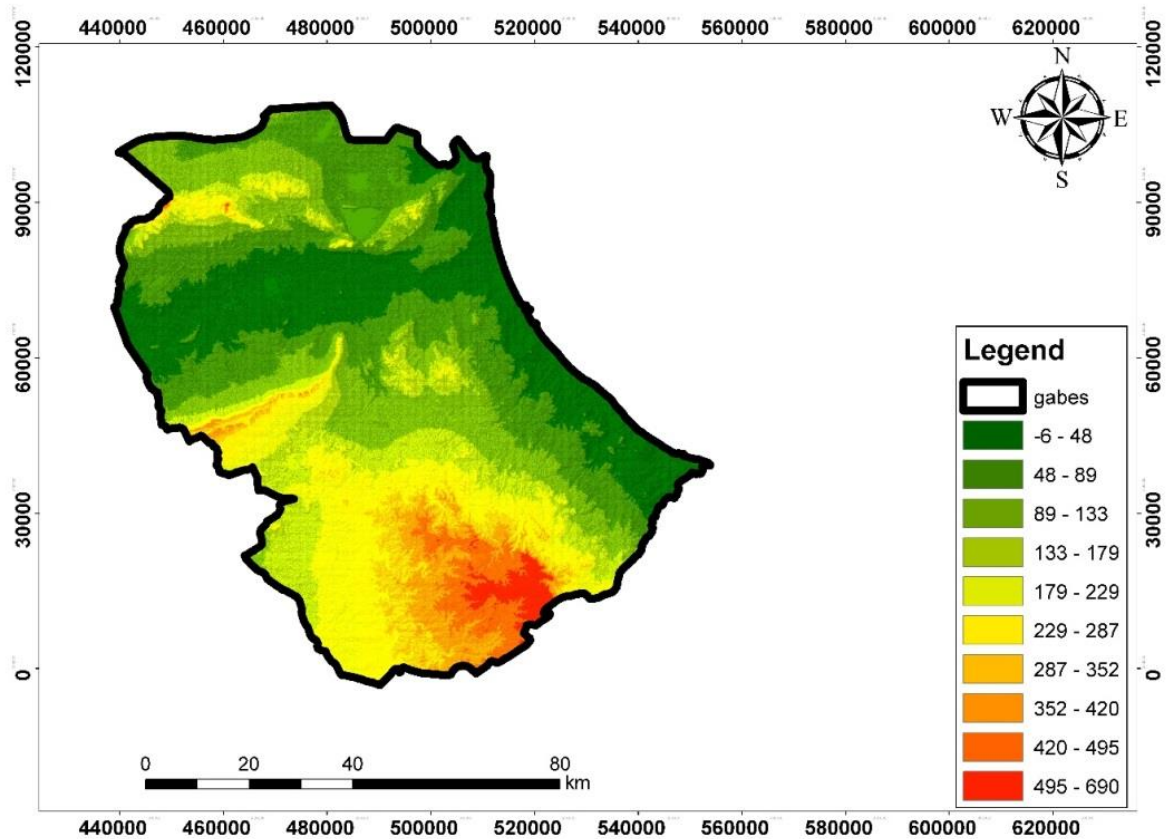


285

286 **Fig.7:** Lithology map of Gabes region (CRDA.2018)

287 **Geomorphology**

288 It is seen from figure 8 that plains and low landforms dominate the Gabes region's topography,  
 289 with a relief ranging from 165 to 605 meters above sea level. Mountains and high landforms  
 290 characterize the southern portion of the research region as well from the north. Based on the  
 291 geomorphology study, Gabes region show a plains in the mostly area in which the recharge  
 292 phenomena can have a good rate. Furthermore in a wide part of study area, these characteristics  
 293 may favorite the composition of wind deposits; floodplain deposits and salt evaporate deposits.  
 294 These variation in the geomorphology character proved a lateral contrast in the potential  
 295 recharge area.



296

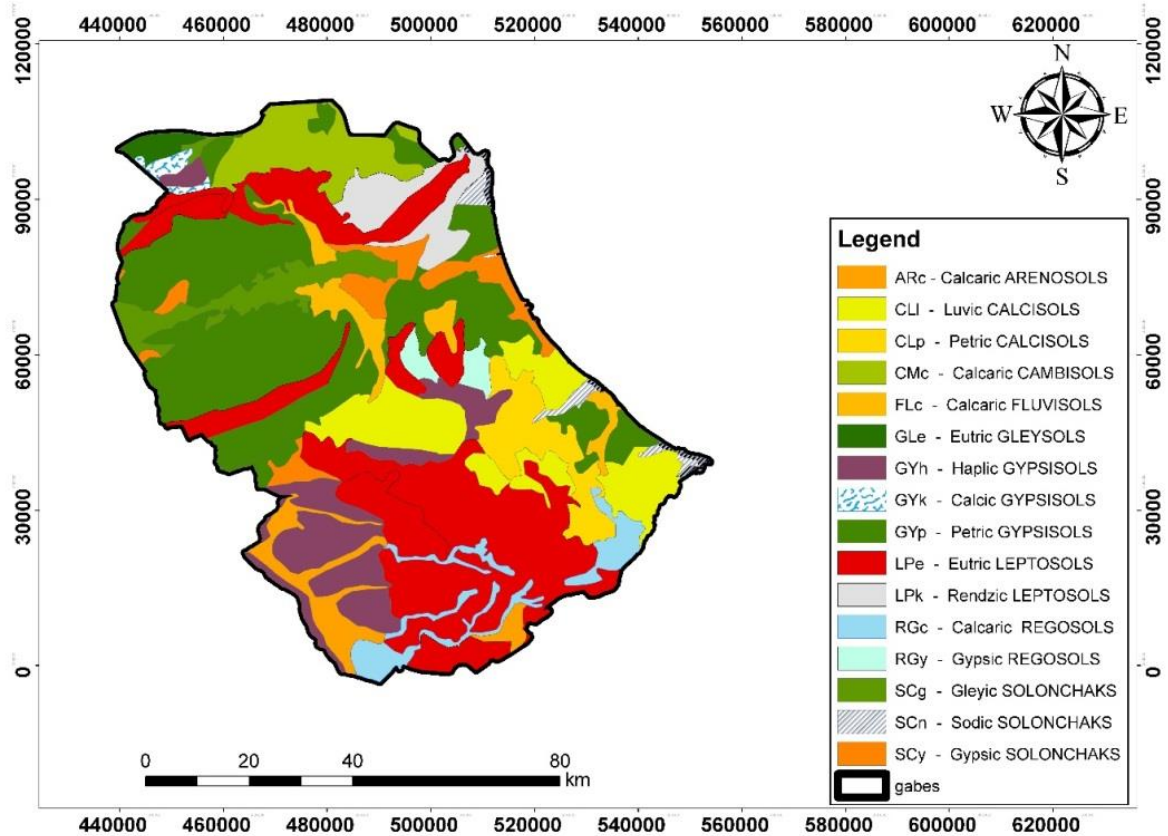
297

**Fig. 8:** Geomorphology map of study area

298

299 **Soil type's factor**

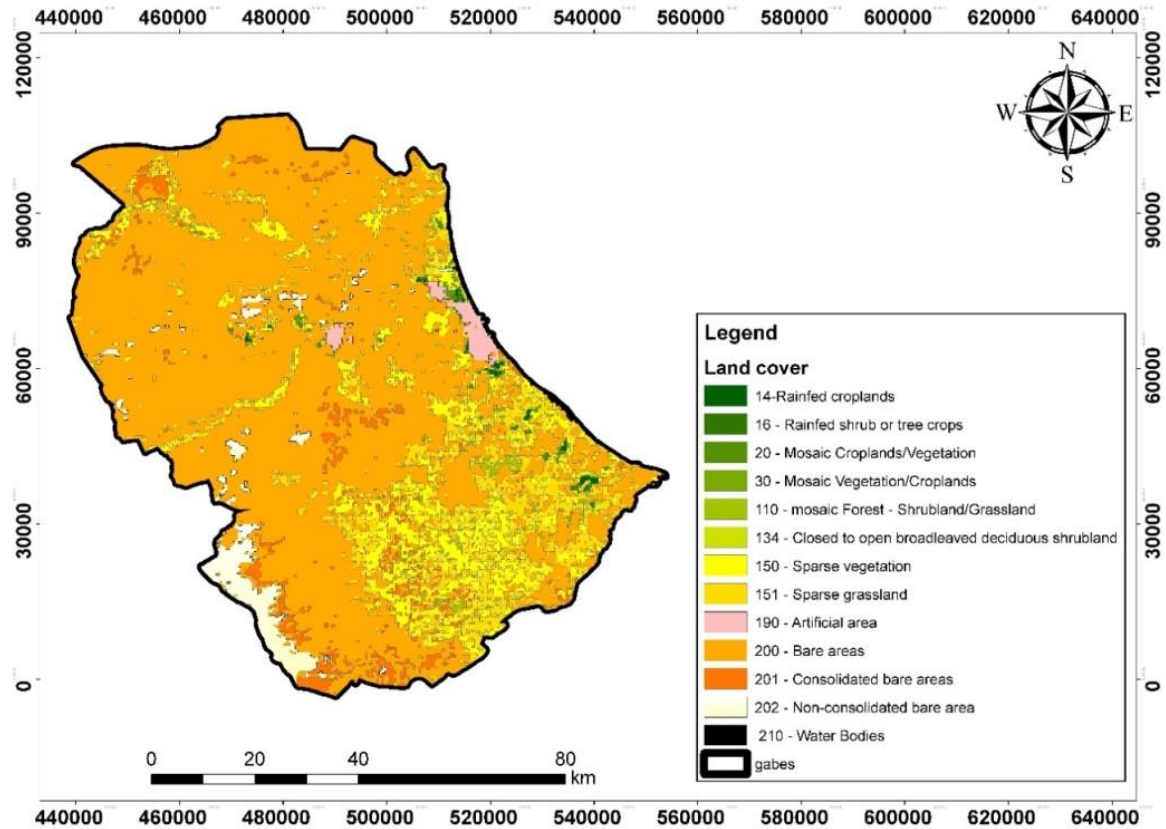
300 It is shown from Figure 9 that the study area present a different soil types. The most of the area  
 301 are covered by sandy-clay/sandy-silty soils, calcic soils and evaporitic. Thus, that variation  
 302 provide the physic characteristic of each type such as permeability and porosity (Ben Baccar  
 303 1982, Alaya et al. 2014) .based on those characteristic the recharge rate faces a very important  
 304 contrast all over the study region giving a point of view about the potential zone that can be  
 305 managed.



306  
307  
308 **Fig. 9.** Soil types map of the Gabes region  
309  
310  
311

### 312 **Land cover**

313 Based on figure 10, the mostly of the study area is exposed land (more than 70% of the study  
314 area), where 10 % of the region is covered by farming lands and sparse vegetation. That  
315 poverty of Greenland have a very important influence on the climate change in the region  
316 (Zheng et al 2019).the vegetation loss has many bad impact such as the raise of temperature  
317 degree . This later push the evapotranspiration rate minimizing the recharge phenomena. As  
318 presenting in the figure 8 that lateral variation of land cover can create a micro-climate like  
319 the oasis. Those characteristic influence the classification of potential recharge area (yeh et al  
320 2009, Malki et al2017)



321

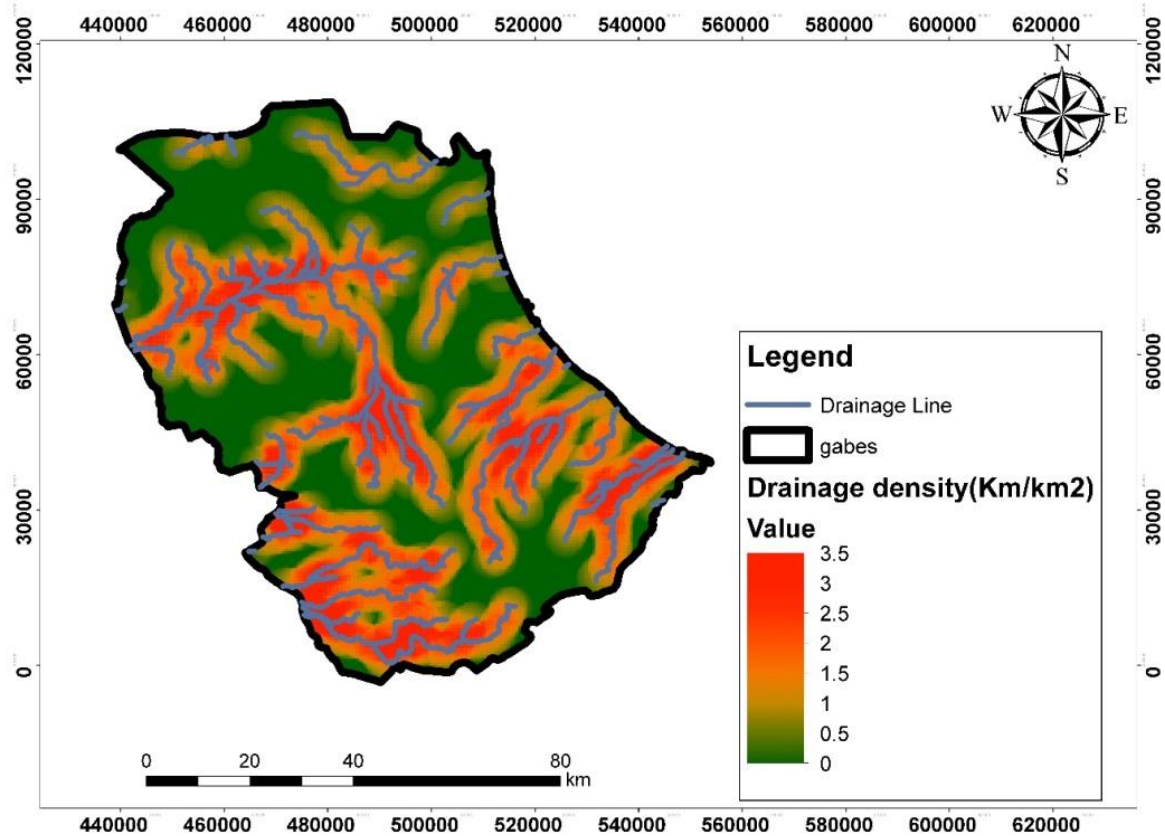
322

**Fig. 10** Land cover of the Gabes region

323

324 **Drainage density**

325 The drainage network in Gabes region was detonated used the used the SRTM. The most  
 326 important flows are located in the south part of the stud region such as the Jir wadis, Segui  
 327 wadis and the Zigzaw wadis. In addition, we found as well the Akarit wadis and the Elhamma  
 328 wadis in the north part. Those wadis are decomposed in tow category endorhic (Elhamma  
 329 wadis) and exoreic (Zigzaw wadis). The density of drainage is varied between [0-3.5 km/km<sup>2</sup>]  
 330 .The Density where they are larger than 1.5 km/km<sup>2</sup>, presented as a region with excellent  
 331 recharge zone .those area present around 30% of the region. The evaluation of drainage density  
 332 map is shown in Fig. 11.



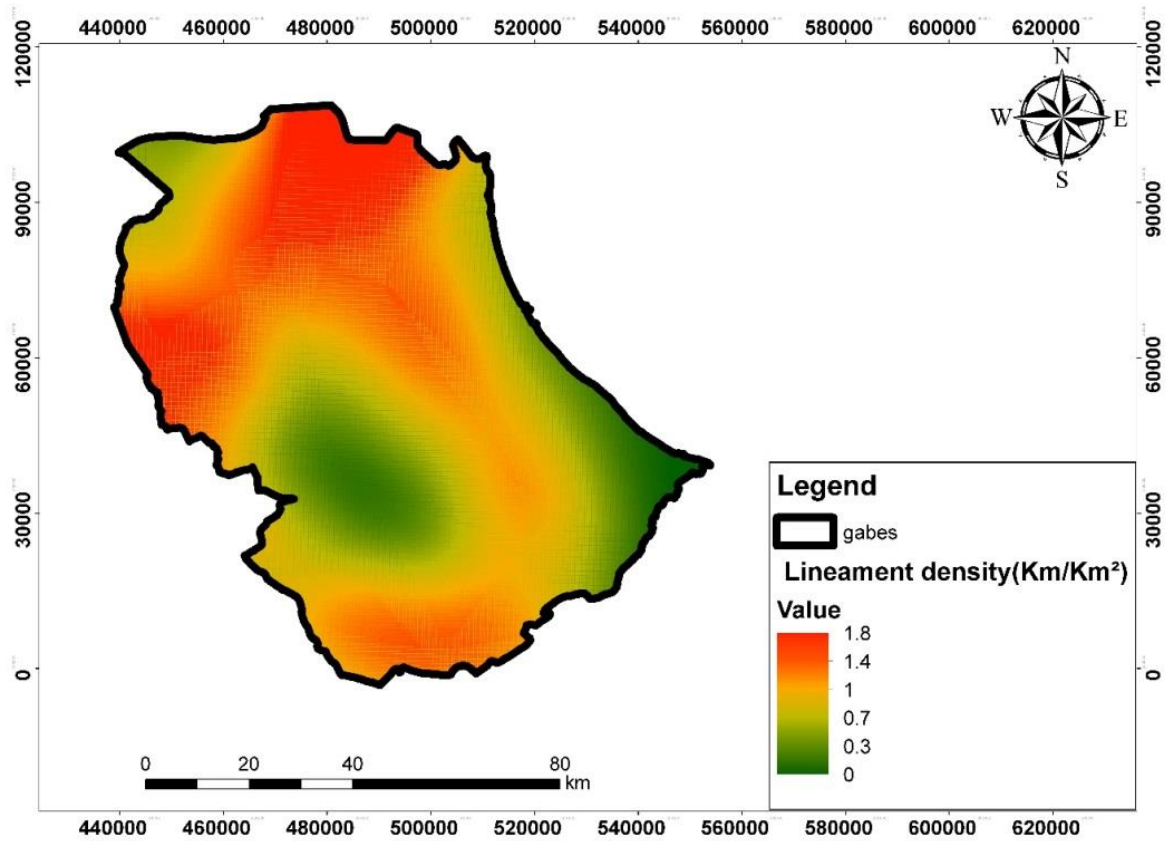
333

334

**Fig. 11** Map of Gabes drainage density

335 **Analysis of lineament density**

336 In order the evaluation of the lineaments in Gabes region, the study based on the SRTM data  
 337 an geological maps of the study region. The result was verified onsite and by bibliography  
 338 (Alaya et al 2014, Zouaghi 2011). The density map was obtained by ArcGIS10.8. The most  
 339 important values is located in the north zone and in the mountainous area, may related the higher  
 340 elevation of those area. More than 50% from the cases study present a value, more than  
 341  $1\text{km}/\text{km}^2$ . The lineament density (Fig. 12) for the Gabes area indicates that the relief has a high  
 342 lineament density, with values varying from 1 to  $1.8\text{ km}/\text{km}^2$ . The lineaments analyses presents  
 343 clearly demonstrate the superiority of a major NNW–SSE lineament course. This correlates to  
 344 the general position of deformation stress associated with the Miocene compressive tectonic  
 345 process (Zargouni 1985, Dlala 1995).



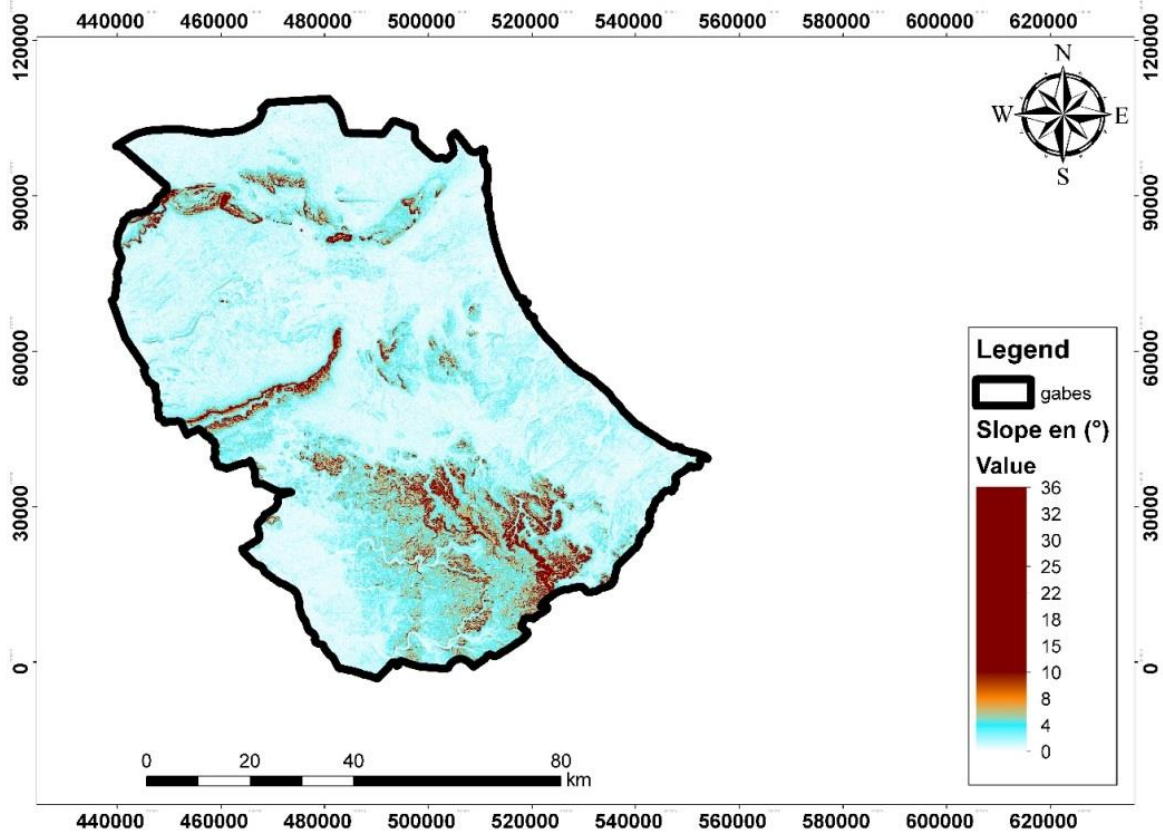
346

347

**Fig. 12** Lineament density map of the study area

348 **Slope**

349 The assessment of the slope evolution in the study area was done based on the MNT treated  
 350 by GIS tools. As shown the generated maps (fig.13), the Gabes region was split into three  
 351 topographic levels based on the slope diagram. The first level (0–2) is assigned to very good  
 352 class which my ameliorate the infiltration ( present the most of the study region ) ; the second  
 353 level (2–4) are rated as moderate groundwater recharge, while the third level is classified as  
 354 having an intensity of 4–10, suggesting a poor groundwater potential recharge.



355

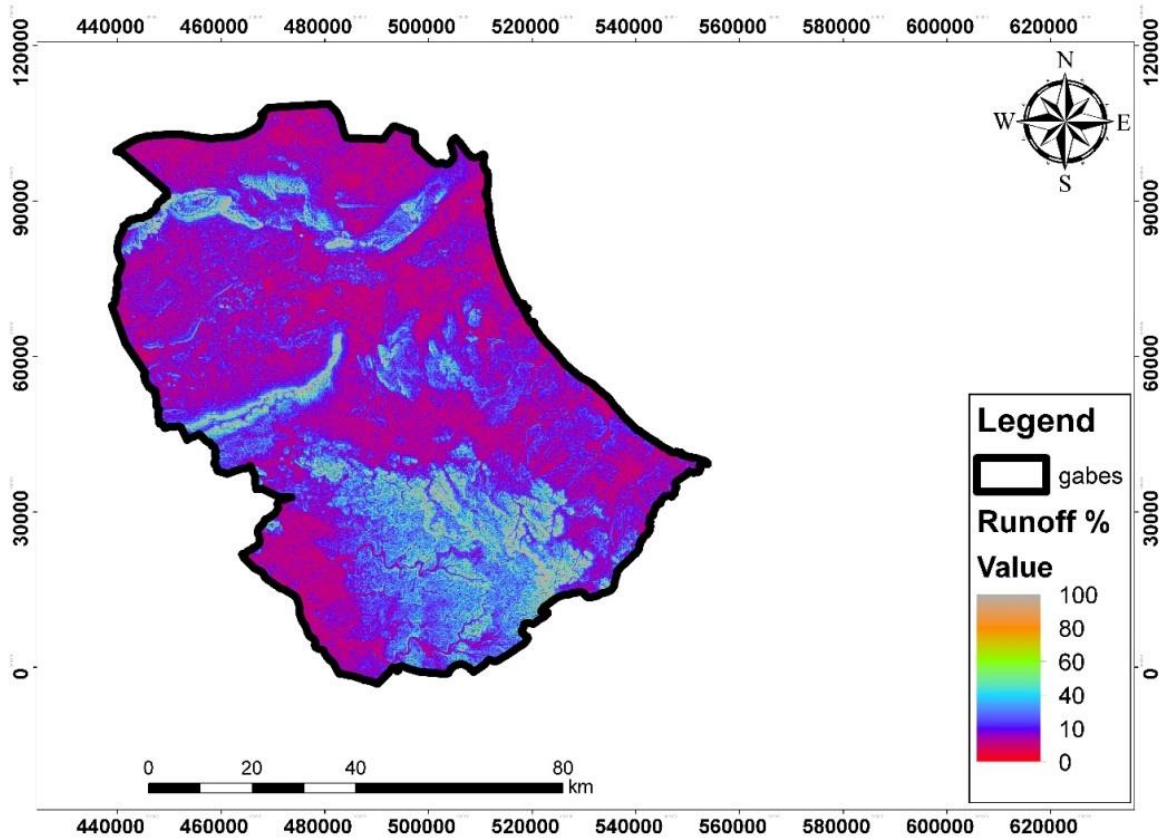
356

**Fig.13** slope map of the study area

357 **Runoff**

358 The study area is categorized into five classes on the basis of runoff map (Fig. 14). Very good  
 359 groundwater potential recharge is assigned to the first class (<4%). This class is located in flat  
 360 terrain; the second category (4–20%), considered as good for groundwater recharge. The third  
 361 category (20–35%), is a moderate recharge area. However, the rest of classes exceeding 35%  
 362 and considered as poor potential groundwater recharge area.

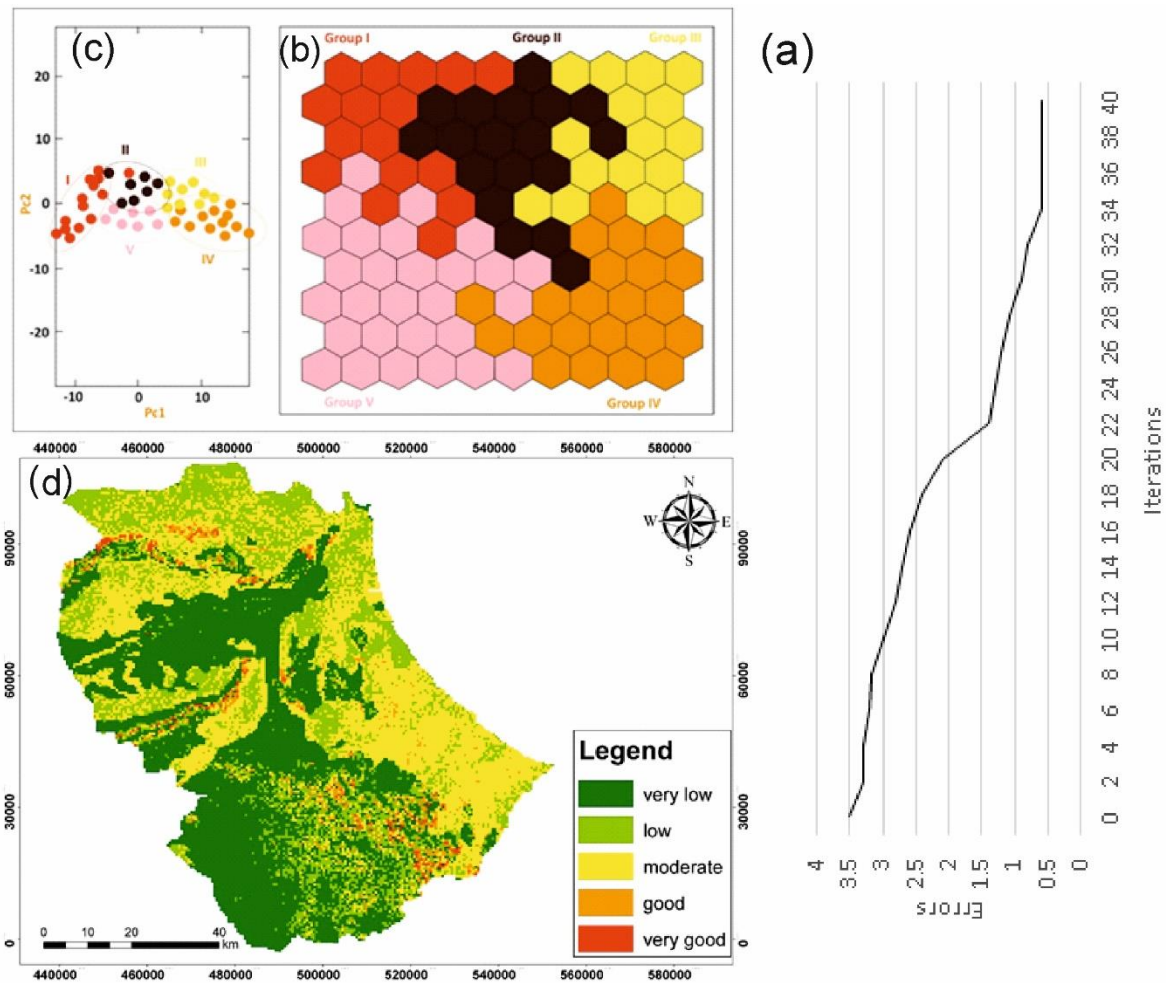
363



364  
365 **Fig. 14** Runoff map of the Gabes region  
366

367  
368 **Potential groundwater recharges areas assessment**

369  $\kappa$ -SOM has been performed using the various parameter that were indicated above from study  
370 area. Kohonen's self-organizing map was realized using SOM Matlab toolbox (Vesanto et al.  
371 1999). Learning was realized until the quantization error after each time has been minimized.  
372 The KSOM quantification error (Fig.15a) shows that the error was stabilized in minimum  
373 values after 40 iterations. The k-SOM analysis results of clustered recharge data from the study  
374 area into five classes from very low to very good recharge potential zones. Those five classes  
375 were validated by the principal parameters analysis resulting of K-SOM (Fig. 15.b,c).



376

377 **Fig. 15:** K-SOM analysis results of potential groundwater zones in study area. (a) SOM quantification  
 378 error after iteration, (b) Principal components, (c) K-SOM maps of obtained classes,(d) spatial  
 379 distribution of groundwater potential zones in the study area

380

381 The five groundwater recharge classes were identified was presented as a map shown the lateral  
 382 variation of those classes (fig.15, d). The first class is very low recharge and represents 27% of  
 383 total surface of study area. The second is a low recharge area and occupies a 23% of study area,  
 384 the third is about 40% of the surface and considered as moderate recharge, however the 7% is  
 385 a good potential recharge and the fifth class has a very high potential recharge and represent  
 386 only 3 % of the total surface of study area. The hydrogeomorphological settings of study area  
 387 reveal that the alluvial plain in the central basin has great groundwater potential to promote  
 388 water infiltration characterized by lower slope, high permeability, and high infiltration rate. As

389 for the mountainous and the hilly sites, located to the southern and western part of the study  
 390 area, have limited potential recharge due to the low infiltration rate. The most important feeding  
 391 area in the Gabes region is characterized by the interrelation of geological and  
 392 geomorphological factors where the low slopes and the intrusion rate are very important, as  
 393 well as the presence of ground cover that can enhance recharge rates, Whereas, the northern  
 394 mountain chain is a faulted zone showing a very good potential recharge indicator. The most  
 395 part of study area is a platform and coastal areas have a moderate recharge index due to the low  
 396 lineament density and drainage as well as the influence of the land cover/use which has a bad  
 397 impact on the groundwater recharge (table 3). The rest of the region presents the association of  
 398 the same factors inducing a low and a very low potential groundwater recharge.

399 **Table 3** Groundwater potential recharge estimation in the study area

Class	Very low	low	moderate	Good	Very good
Area (km <sup>2</sup> )	1933.2	1648.18	2866	501.02	214.88
Average %	27	23	40	7	3
Potential recharge (m <sup>3</sup> .y <sup>-1</sup> )	3093120	2637088	4585600	801632	343808
Total of recharge (m <sup>3</sup> .y <sup>-1</sup> )	11461248				

400  
 401 Quantifying groundwater recharge in southern Tunisia using hydrological and hydrodynamic  
 402 models is a difficult task. Baba-Sy (2005) has indicated that infiltration rate varies between 2  
 403 and 10% in southern Tunisia. Consequently, infiltration is of 7 to 12 mm/year, which is  
 404 estimated to 5 to 8% of annual precipitation. For potential groundwater recharge estimation in  
 405 Gabès region, on the basis of Fersi (1979) findings, an infiltration rate of 8% from the annual  
 406 precipitation of 200 mm.y<sup>-1</sup>, potential groundwater recharge is estimated to 11461248 m<sup>3</sup>.y<sup>-1</sup>.  
 407 For a given hydrogeological system, the identification of the potential recharge zone using the  
 408 RST can be used to translate several variables into one basic criterion to determine the proposal

409 recharge zone. The RST provided as flexible approach fir adding or changing parameters. This  
410 method are using by several researches (yeh et al 2016, Yahyaoui et al 2021). Suissi et al 2018  
411 was applied that method in same study region integrating a various parameters while reducing  
412 possibility of errors. Varaiious are the study that based on the remote sensing technique but use  
413 of RST copulate with K-SOM method was so limited. In according with earlier studies (yeh et  
414 al 2016; Yahyaoui et al . 2017), the RST copulated with the self-organizing maps in this study  
415 used to evaluate the lateral variation of potential recharge zone in arid area specially in Gabes  
416 region . This method is robust and flexible with the criteria, as well it can be applied in many  
417 domain and in another study area .

## 418 **5. Conclusion and recommendation**

419 In this works, the recharge process was assessed to determine the potential recharge zone in  
420 Gabes region in order to purpose a required strategy to ameliorate the recharge phenomena,  
421 based on RST and K-SOM. This method used to define the weights of different criteria (slope,  
422 lithology, geomorphology, drainage, lineaments, land cover /user...). Groundwater potential  
423 zone is classed in five classes (very good, good, moderate, low and very low). The most part of  
424 the Gabes region are classed as moderate. The results confirmed that the Gabes region has a  
425 medium recharge potential, with 10% of the total area representing a high recharge while the  
426 rest of the region has a medium to very low recharge potential. The estimated potential  
427 groundwater recharge in Gabès region is of 11, 46 Mm<sup>3</sup>/year. Additionally, a study of the impact  
428 of climate change on the amount and recharge process available in this region associate with an  
429 isotopies study would be a major aid to decision making at the local level.

430

## 431 **Declarations**

432 **Conflict of interest** the authors declare no competing interests.

433 **Foundation** The authors declare that this work has no foundation support.

434

435 **References**

436 Abdallah, H., Memmi, L., Damotte, R., Rat, P., & Magniez-Jannin, F. (1995). Le Crétacé de la  
437 chaîne nord des Chotts (Tunisie du centre-Sud): biostratigraphie et comparaison avec les  
438 régions voisines. *Cretaceous Research*, 16(5), 487-538 (in French)

439 Abdollahi K. (2015). Basin scale water balance modeling for variable hydrological. *African*  
440 *Earth Sciences*, 132 :37–46.

441 Agoubi B, (2021) . A review: saltwater intrusion in North Africa’s coastal areas - current state  
442 and future challenges. *Environ Sciences Pollution Res.* (28):17029–17043.  
443 <https://doi.org/10.1007/s11356-021-12741-z>

444 Agoubi B. (2018). Assessing hydrothermal groundwater flow path using Kohonen’s SOM,  
445 geochemical data, and groundwater temperature cooling trend. *Environmental Science*  
446 *and Pollution Research*. <https://doi.org/10.1007/s11356-018-1525-1>

447 Agoubi B., Kharroubi A. et Abida H. (2012). Saltwater intrusion modelling in Jorf coastal  
448 aquifer, South-eastern Tunisia: Geochemical, geoelectrical and geostatistical application.  
449 *Hydrol. Process journal*. DOI: 10.1002/hyp.

450 Akbari, M., Alamdarlo, H. N., & Mosavi, S. H. (2020). The effects of climate change and  
451 groundwater salinity on farmers’ income risk. *Ecological Indicators*, 110, 105893.

452 Al Saud M. (2010). Mapping potential areas for groundwater storage in Wadi Aurnah Basin,  
453 western Arabian Peninsula, using remote sensing and geographic information system  
454 techniques. *Hydrogeology journal*, 18(6), 1481-1495. and *Hydraulic Engineering*, Vrije  
455 Universiteit Brussel, Brussels, Belgium, p 173.

456 Arulbalaji P., D. Padmalal and K. Sreelash, (2019). AHP and GIS based delineation of  
457 groundwater potential areas. *Scientific Reports (9):2082*, [https://doi.org/10.1038/s41598-](https://doi.org/10.1038/s41598-019-38567-x)  
458 [019-38567-x](https://doi.org/10.1038/s41598-019-38567-x)

459 Awadh, S. M., Al-Mimar, H., & Yaseen, Z. M. (2021). Groundwater availability and water  
460 demand sustainability over the upper mega aquifers of Arabian Peninsula and west region  
461 of Iraq. *Environment, Development and Sustainability*, 23(1), 1-21.

462 Baba-Sy J. (2005). Recharge of the aquifer system of the north Sahara. Published PhD thesis.  
463 University of Tunis.

464 Balamurugan G, Karthik S, Somnath B (2017). Frequency ratio model for groundwater  
465 potential mapping and its sustainable management in cold desert, India. *J King Saud Univ*  
466 *- Sci* 29(3):333–347

467 Ben Alaya M., S. Saidi, T. Zemni, F. Zargouni (2013). Deep-groundwater Assessment for  
468 drinking and irrigation use, Djefara aquifers, Southeastern Tunisia. *Env. Earth Sci*  
469 (71):3387–3421. <https://doi.org/10.1007/s12665-013-2729-9>

470 Ben Hamouda M.F., A. Mamou, J. Bejaoui, K. Froehlich (2013). Hydrochemical and Isotopic  
471 Study of Groundwater in the North Djefara Aquifer, Gulf of Gabès, Southern Tunisia.  
472 *International Journal of Geosciences*, Vol. 4, No. 8A, p:1-10;  
473 [DOI:10.4236/ijg.2013.48A001](https://doi.org/10.4236/ijg.2013.48A001)

474 Bouaziz S, Barrier E, Soussi M, Turki MM, Zouari H (2002) Tectonic evolution of the northern  
475 African margin in Tunisia from paleostress data and sedimentary record. *Tectonophysics*  
476 357:227–253

477 Bouaziz S. (1995). Study of tectonics in the Saharan platform and Atlas (southern Tunisia):  
478 evolution of paleo-fields of constraints and geodynamic implications. PhD Thesis,  
479 University of Tunis.

480 Bouderbala, A. (2019). The impact of climate change on groundwater resources in coastal  
481 aquifers: case of the alluvial aquifer of Mitidja in Algeria. *Environmental Earth*  
482 *Sciences*, 78(24), 1-13.

483 Cereghino R., Y. Park (2009). Review: the self-organizing map approach in water resources.  
484 *Environ Model Software* (24):945–947. <https://doi.org/10.1016/j.envsoft.2009.01.008>

485 Choi, W., Galasinski, U., Cho, S. J., & Hwang, C. S. (2012). A spatiotemporal analysis of  
486 groundwater level changes in relation to urban growth and groundwater recharge  
487 potential for Waukesha County, Wisconsin. *Geographical Analysis*, 44(3), 219-234.

488 Clark S. (2018). Advance in SOM for spatiotemporal and nonlinear system. Doctorate of Philosophy,  
489 University of New South Wales, Sydney, Australia. 190p  
490 (<https://unsworks.unsw.edu.au/fapi/datastream/unsworks:52796/SOURCE02?view=true> ,  
491 visited the August 9, 2021)

492 Dar T., N. Rai, A. Bhat (2020). Potential groundwater recharge zones delineation using AHP.  
493 *Geology, and Landscapes* :1–16. <https://doi.org/10.1080/24749508.2020.1726562>

494 Dlala M., (1995). Evolution géodynamique et tectonique superposées en Tunisie : implication  
495 sur l'évolution géodynamique récente et la sismicité. Thèse En Sciences Géologique.  
496 Université de Tunis El Manar II

497 El Baz F., (1995). Groundwater potential recharge of the Sinai Peninsula in Egypt. Boston,  
498 Center for Remote Sensing.

499 Foster S., D.P. Loucks (2006). A guide-book on sustainable management of water policy  
500 makers. I.H.P Groundwater series, (10). Paris: UNESCO

501 Freeze, R. and Cherry, J. (1979). Groundwater, Englewood Cliffs, New Jersey 07632.  
502 <http://hydrogeologistswithoutborders.org/wordpress/1979-english/>, accessed June 17,  
503 2021)

504 Gude, V. G. (2018). Desalination of deep groundwater aquifers for freshwater supplies–  
505 Challenges and strategies. *Groundwater for Sustainable Development*, 6, 87-92.

506 Haridas V.R., S. Aravindan, G. Girish (1998). Remote sensing and applications for groundwater  
507 favorable areas identification. *Quarterly Journal* (6), 18–22.

508 Huang C., H.F. Yeh, H.I. Lin, S.T. Lee, K.C. Hsu, C.H. Lee (2013). Ground water recharge  
509 and exploitative potential zones using GIS and GOD. *Envir. Earth Sci.*, (68): 267–280.  
510 doi:10.1007/s12665-012-1737-5

511 Kangur K, Park Y-S, Kangur A, Kangur P, Lek S (2007) Patterning longterm changes of fish  
512 community in large shallow Lake Peipsi. *Ecol Model* 203:34–44

513 Kohonen T. (1982) SOM formation of topological correct feature maps. *Biol Cybern* (43):59-  
514 69

515 Kulmatov, R. A., Adilov, S. A., & Khasanov, S. (2020, December). Evaluation of the spatial  
516 and temporal changes in groundwater level and mineralization in agricultural lands under  
517 climate change in the Syrdarya province, Uzbekistan. In *IOP Conference Series: Earth  
518 and Environmental Science* (Vol. 614, No. 1, p. 012149). IOP Publishing.

519 Kumar P.K., G. Gopinath, P. Seralathan P. (2007). Application of RS and GIS for delineation  
520 of groundwater potential zones: River basin in Kerala, southwest India. *Intern. Jour.  
521 Remote Sensing* (24), 5583–5601. Doi:10.1080/ 01431160601086050

522 L-Baz, F., et al., (1995). Groundwater potential of the Sinai Peninsula, Egypt. Project Summary.  
523 Boston, RS Center.

524 Leduc C., Favreau G., Schroeter P. (2001). Long-term rise level in a Sahel watertable: The CT  
525 in south-west Niger. *Journal of hydrology*, 243(1-2), 43-54.

526 Lee GF, Jones-Lee A. (1999). Evaluation of surface water quality impacts of hazardous  
527 chemical sites. *Remediation* 9(2):87–113

528 Machiwal D., Jha M.K., Mal B.C (2011). Groundwater potential in a semi-arid region of india  
529 using RS, GIS and MCDM. *Water resources management*, 25 (5), pp:1359-1386.

530 Makni J, Ben Brahim F, Hassine S, Bouri S, Ben Dhia H (2012) Hydrogeological and mixing  
531 process of waters in deep aquifers in arid regions: south east Tunisia. *Arab J Geosci*  
532 6:2673–2683. <https://doi.org/10.1007/s12517-011-0510-5>

533 Mamou A. (1990). Characteristics and Evaluation of water Resources in Southern Tunisia. PhD thesis,  
534 University of South-Paris, 425 p.

535 Melki A., Abdollah K., Fatahi R., and Abida H. (2017). Groundwater recharge estimation under  
536 semi-arid climate : Case of northern gafsa watershed, Tunisia. *Journal of African Earth*  
537 *Sciences*, Volume 132, 37-46, <https://doi.org/10.1016/j.jafrearsci.2017.04.020>

538 Mishra R.C., Biju C., Ranjitsingh D.N. (2010). Remote sensing and GIS for groundwater  
539 mapping and identification of artificial recharge sites. *Geo Shanghai Inter. Conference:*  
540 216–223

541 Nadiri, A. A., Norouzi, H., Khatibi, R., & Gharekhani, M. (2019). Groundwater DRASTIC  
542 vulnerability mapping by unsupervised and supervised techniques using a modelling  
543 strategy in two levels. *Journal of Hydrology*, 574, 744-759.

544 Oikonomidis D. (2015). GIS and RS methodology for groundwater assessment in Tirnvos  
545 area, Greece. *Journal of Hydrology* (525):197-208. doi:10.1016/j.jhydrol.2015.03.056

546 Ousmana H, El Hmaid A, Berrada M, Damnati B, Etebaai I (2016). Application of the self  
547 organizing map method for the classification of the environmental quality of the lake

548 systems in the moroccan middle atlas: lakes cases of Ifrah, Iffer and Afourgagh. Larhyss  
549 Journal, ISSN 1112–3680, n°25, pp. 49–65

550 Parkinson, S., & Hunt, J. (2020). Economic potential for rainfed agrivoltaics in groundwater-  
551 stressed regions. *Environmental Science & Technology Letters*, 7(7), 525-531.

552 Pool, S., Francés, F., Garcia-Prats, A., Pulido-Velazquez, M., Sanchis-Ibor, C., Schirmer, M.,  
553 ... & Jiménez-Martínez, J. (2021). From flood to drip irrigation under climate change:  
554 Impacts on evapotranspiration and groundwater recharge in the Mediterranean region of  
555 Valencia (Spain). *Earth's Future*, 9(5), e2020EF001859.

556 Sahli H, Tagorti M A, Tlig S, (2013). Groundwater hydrochemistry and mass transfer in  
557 stratified aquifers system (Jeffara Gabes basin, Tunisia). *Larhyss Jpurnal*, 12, pp. 95-108.

558 Shrestha, S., Neupane, S., Mohanasundaram, S., & Pandey, V. P. (2020). Mapping groundwater  
559 resiliency under climate change scenarios: A case study of Kathmandu Valley,  
560 Nepal. *Environmental research*, 183, 109149.

561 Singh S.K., M. Zeddies, U. Shankar, G.A. Griffiths(2019). Potential groundwater recharge  
562 zones in New Zealand. *Geosci Front* 10:1065-1072

563 Trabelsi, R. (2006). *Approche itérative d'homogénéisation pour le comportement des*  
564 *composites polydisperses: applications à l'endommagement des mousses syntactiques*  
565 *immergées* (Doctoral dissertation, Paris 6).

566 UNESCO (2019). *The United Nations World Water Development Report. Executive Summary,*  
567 *15p. (<https://unesdoc.unesco.org/ark:/48223/pf0000367303>, visited the June 15, 2021)*

568 Vesanto J., E. Alhoneim E, (2000). Clustering of the S.O.M., *IEEE Trans Neural Networks*, 11:  
569 586–600

570 Walter, J. (2018). Modèle d'évolution naturelle de l'eau souterraine dans une région du  
571 Bouclier Canadien à partir de la détermination de pôles hydrogéochimiques  
572 régionaux (Doctoral dissertation, Université du Québec à Chicoutimi).

573 Yahiaoui B., B. Agoubi, A. Kharroubi (2021). Groundwater potential recharge areas delineation  
574 using GPRI index: Ghomrassen, south Tunisia. AJGS journal,14:919 ;  
575 <https://doi.org/10.1007/s12517-021-07173-5>

576 Zargouni F (1985) Tectonique de l'Atlas Méridional de Tunisie: évolution géométrique et  
577 cinématique des structures en zone de cisaillement. Rev Sci Terre 3:304p

578 Zargouni, F., 1985. Tectonics of the Southern Atlas of Tunisia. Geometric and kinematic  
579 evolution of structures in shear zones. Thesis in Sciences. Louis Pasteur University,  
580 Strasbourg, France, 296 (In French).

581 Zheng, K., Wei, J. Z., Pei, J. Y., Cheng, H., Zhang, X. L., Huang, F. Q., ... & Ye, J. S. (2019).  
582 Impacts of climate change and human activities on grassland vegetation variation in the  
583 Chinese Loess Plateau. Science of the Total Environment, 660, 236-244.

584 Zouaghi T, Guellala R, Lazzez M, Bédir M, Ben Youssef M, Inoubli MH, Zargouni F (2011)  
585 The chotts fold belt of southern Tunisia, North African margin, structural pattern, evolution  
586 and regional geodynamic implications. In: Schattner U (ed) New frontiers in tectonic  
587 research—At the midst of plate convergence. InTech. ISBN 978-953-307-594-5

588